Building and Environment 224 (2022) 109530

Contents lists available at ScienceDirect

Building and Environment

journal homepage: www.elsevier.com/locate/buildenv

Ceiling impact on air disinfection performance of Upper-Room Germicidal Ultraviolet (UR-GUV)

Shengwei Zhu [a], Tong Lin [a], Lingzhe Wang [a], Edward A. Nardell [b], Richard L. Vincent [c], Jelena Srebric [a,*]

[a] Department of Mechanical Engineering, University of Maryland, College Park, MD, USA
[b] Departments of Environmental Health and Immunology and Infectious Diseases, Harvard T.H. Chan School of Public Health, Boston, MA, USA
[c] Icahn School of Medicine Mount Sinai, New York City, NY, USA

ARTICLE INFO

Keywords:
Computational Fluid Dynamics (CFD)
Upper-Room Germicidal Ultraviolet (UR-GUV)
Filtration
COVID-19
Airborne infection
Ceiling height

ABSTRACT

This study used Computational Fluid Dynamics (CFD) to investigate air disinfection for SARS-CoV-2 by the Upper-Room Germicidal Ultraviolet (UR-GUV), with focus on ceiling impact. The study includes three indoor settings, i.e., low (airport bus), medium (classroom) and high (rehearsal room) ceilings, which were ventilated with 100% clean air (CA case), 80% air-recirculation with a low filtration (LF case), and 80% air-recirculation with a high filtration (HF case). According to the results, using UR-GUV can offset the increased infection risk caused by air recirculation, with viral concentrations in near field (NF) and far field (FF) in the LF case similar to those in the CA case. In the CA case, fraction remaining (*FR*) was 0.48–0.73 with 25% occupancy rate (OR) and 0.49–0.91 with 45% OR in the bus, 0.41 in NF and 0.11 in FF in the classroom, and 0.18 in NF and 0.09 in FF in the rehearsal room. Obviously, UR-GUV performance in NF can be improved in a room with a high ceiling where *FR* has a power relationship with UV zone height. As using UR-GUV can only extend the exposure time to get infection risk of 1% ($T_{1\%}$) to 8 min in NF in the classroom, and 47 min in NF in the rehearsal room, it is necessary to abide by social distancing in the two rooms. In addition, $T_{1\%}$ in FF was calculated to be 18.3 min with 25% OR and 21.4% with 45% OR in the airport bus, showing the necessity to further wear a mask.

1. Introduction

People are much more likely to get infected with COVID-19 by the inhalation of SARS-CoV-2 carried by aerosols (≤5 μm [1]) than by the SARS-CoV-2 carried by large droplets, typically deposited onto the mucous membranes in eyes, nostrils, or lips [2]. Talking and breathing generates aerosols capable of efficient COVID-19 spread [3,4] because SARS-CoV-2 can be transmitted between people via the exhaled viral aerosols in both short- and long-range, also called near- and far-fields [5].

Mechanical ventilation is typically designed for occupant comfort, such as the removal of odor and air pollutants, and temperature and humidity control, not for airborne infection control. The exception are health-care facilities that can supply a minimum of 6–12 room air changes per hour (ACH) recommended for airborne infection control [6]. Importantly, several recent studies established a contributing role of insufficient ventilation to indoor COVID-19 transmission in public spaces, such as bars, churches, restaurants, and buses [7–12]. Filtration has been widely applied in the existing central heating, ventilation, and air-conditioning (HVAC) systems to clean the recirculated air. Although a high efficiency particulate air (HEPA) filter is able to remove at least 99.97% of all particles that are 0.15–0.2 μm [13], its use is not feasible in many existing HVAC systems due to its high resistance to air from circulation [14]. In practice, it is a MERV 13 (Minimum Efficiency Reporting Value) filter, not a HEPA filter, that is recommended for U.S. public buildings for control of SARS-CoV-2 airborne transmission [15–17]. Furthermore, in some special indoor settings, such as buses, filters were upgraded to a MERV 8 or even lower because of the relatively large ACH rates in transportation vehicles [18]. Note that a MERV 8 filter is not able to remove particles less than 3 μm, and a MERV 13 can only remove <75% of the particles smaller than 1 μm [19]. These limitations indicate additional air cleaning measures to control the COVID-19 spread of tiny particles which are impossible to be fully removed by these filters.

Upper-Room Germicidal UV (UR-GUV) technology [20] has been proven an effective whole-room air and surface disinfection measure

* Corresponding author. Technology Ventures, Building Suite 4403, 5000 College Ave. College Park, MD, 20740-3809, USA.
E-mail address: jsrebric@umd.edu (J. Srebric).

https://doi.org/10.1016/j.buildenv.2022.109530
Received 30 June 2022; Received in revised form 12 August 2022; Accepted 21 August 2022
Available online 31 August 2022

against COVID-19 spread in hospitals [21], and is a recommended measure for the prevention of COVID-19 transmission [22,23]. An UR-GUV system includes one or several UV fixtures suspended from the ceiling or mounted on a wall, which use parallel louvers to deflect UV light to the upper room overhead, and generate a UV irradiation zone with a high irradiance level (UV zone). With UR-GUV, the irradiance level is limited in the lower room (occupied zone) to prevent overexposure to UV irradiation, which may cause erythema to the skin and photokeratitis to the eyes [24].

Rooms with a ceiling height less than 2.3 m are usually not equipped with UR-GUV due to possible ceiling reflectance into the occupied zone [25]. Therefore, because of height limitations thus far, UR-GUV has rarely been applied to ground transportation vehicles, such as buses and trains, where there is a low overhead space but crowded. In contrast, high ceilings (≥2.7 m) enable the use of unshielded UV lamps (without louvers) [25] to provide a higher irradiance level. Because of little experience in applying UR-GUV in high-ceiling indoor spaces, the sensitivity of its performance is unclear at the elevation and height of the UV zone where the air is not well mixed.

Our previous studies demonstrated that Computational Fluid Dynamics (CFD) is capable of evaluating UR-GUV air disinfection performance [26–28]. In this study, we developed the CFD method to integrate simultaneous analyses of air recirculation, particle filtration, and UR-GUV air disinfection with the transport process of exhaled aerosols. With this new method, we investigated the UR-GUV application in a classroom with a medium ceiling height (2.74 m), an airport bus with a low ceiling height (2.45 m), and a rehearsal room with an extremely high ceiling (7.47 m). The investigation will include different air-recirculation/filtration conditions to see if using UR-GUV could counterweight the increased infection risk caused by air-recirculation. Furthermore, the investigation will be not limited to the overall infection risk, but also test if this whole-room air disinfection measure is useful for providing protection in the near field (NF) around the index case. Importantly, this study will specifically focus on the impact of ceiling height and available volume when investigating UR-GUV air disinfection performance. In addition, we will clarify if it is still necessary to wear a mask and/or abide by social distancing when using UR-GUV, regarding that there is always resistance to wearing a mask due to social, neurological and psychological factors [29], meanwhile many people won't adhere to all social distancing rules, especially when one is not identified as highly vulnerable to COVID-19 [30].

2. Methodology

We created the CFD models based on the spatial configuration and ventilation design of actual indoor spaces representing an airport bus, a classroom, and a rehearsal room, to investigate the impacts of ceiling height and air disinfection volume on UR-GUV efficacy.

2.1. Room models

This study created four models, including two bus models for an airport bus (Cobus 3000) with occupancy rate (OR) of 25% (27 people) and 45% (50 people), a general classroom with one teacher and 16 students, and a rehearsal room of School of Music with three people. Fig. 1 shows the four models for the three indoor settings. The occupancy in the classroom and rehearsal room was determined according to the administrative regulations during the pandemic, while the bus occupancy was varied from low to high, in the two different bus models. This study conducted the simulations of residual lifetime of air (*RLTa*) [31,32] to determine the index cases for the investigation. *RLTa* at an occupant's mouth opening represents the mean time that his/her

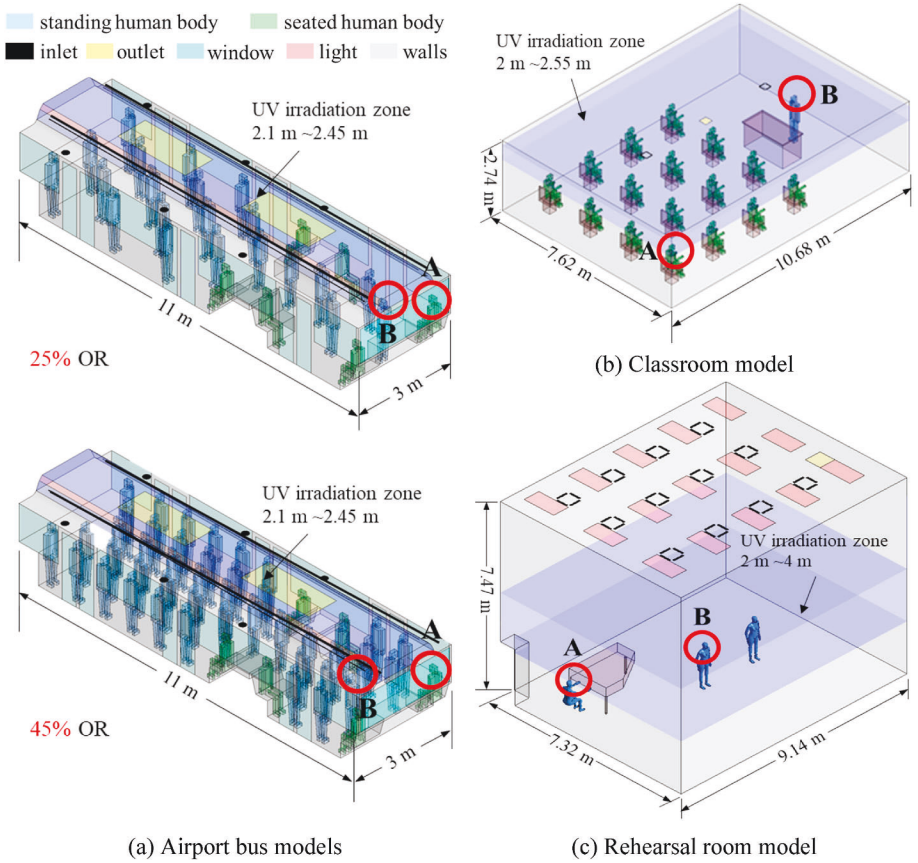

Fig. 1. CFD models for three indoor settings. Red circle highlights the index case. (For interpretation of the references to colour in this figure legend, the reader is referred to the Web version of this article.)

exhaled breath takes to reach the outlet (air return/exhaust). Therefore, a larger *RLTa* value means that the exhaled air will have longer indoor resident time than the breaths of other occupants. As a result, in each model, one seated (A) and another standing (B), whose exhaled breath had the longest indoor resident time among the occupants, were chosen as the index cases for COVID-19. Note that with each model, we simulated flow field and viral spread for each index case. When one index case was simulated, the other one was assumed to be a recipient doing constant inhalation.

This airport bus's air distribution has two linear and six round inlets. The linear inlets at each side close to the ceiling were simplified as rectangular openings with the same length and area as the original design. The six round inlets are symmetrically distributed in the front and middle part at each side, providing more air supply in these areas than the rear part. Air of 20.2 °C [33] is supplied from the normal direction of the inlets, with an air exchange rate of 30 ACH (air change per hour). The airport bus's outlet includes two rectangular openings located in the middle of the ceiling. The airport bus has a concave-upward ceiling between 2.1 m and 2.45 m, which was taken as UV zone in the bus models.

The classroom has two square ceiling diffusers in the front and rear parts and a square outlet at the center of the ceiling. The supplying openings of each diffuser are simplified as four rectangular openings at each side the diffuser, with air supplied at a spread angle of 30°. The rehearsal room has 12 plaque style air diffusers, which were simplified as in the classroom model, but the air was supplied straight downward according to our measurement. There is only one square outlet in the ceiling as shown in Fig. 1(c). According to the campus's administrative regulation, air exchange rate was set to be 3 ACH in the two models, with air temperature to be 22 °C. In the classroom model, the UV zone was located between 2 m and 2.55 m, with a volume of 20% of room space, representing a general application of UR-GUV. For the rehearsal room, we did the simulations with a variety of elevations and heights for UV zone.

For all these models, we consider three ventilation conditions: 1) 100% clean air supply (CA case); 2) 80% air-recirculation with low filtration, i.e., a MERV4 filter for airport bus and a MERV8 filter for classroom and rehearsal room (LF case); and 3) 80% air-recirculation with high filtration, i.e., a MERV8 filter for airport bus and a MERV13 filter for classroom and rehearsal room (HF case). LF case presents the ventilation operation implemented before the COVID-19 pandemic, while HF case for the current ventilation practice. CA case for the ideal conditions with HEPA filter or 100% outdoor air supply.

In the airport bus and classroom models, this study used the simple human body shapes with the rectangles of different sizes to represent body parts, to reduce the complexity of spatial configuration. We first created the simulation domains using tetrahedral meshes, with Aspect Ratio <6.04 and Skewness Equiangle <0.78. After importing the tetrahedral meshes into Fluent, we applied the Polyhedral meshing function to convert the tetrahedral meshes to polyhedral meshes, which could improve mesh quality meanwhile it greatly reduced the cell count. As a result, simulation domain finally had 2.025 M cells for 25% OR bus, 1.36 M cells for 45% OR bus, 1.494 M cells for classroom, and 1.871 M cells for rehearsal room. According to our grid independence study [33] and other similar studies [34,35], these cell counts are sufficient to ensure the grid independence for the models. The polyhedral mesh quality is appropriate for Ansys Fluent, with orthogonal quality of 0.31, 0.33, 0.32, and 0.28 for the 25% OR bus, 45% OR bus, classroom, and rehearsal room models, respectively. Fig. 2 presents an example of meshes across the standing human bodies in the rehearsal room model. To account for the complex body shape, we created additional blocks to refine the meshes around the human bodies.

2.2. CFD approaches

This modeling method validated and used in our previous study on UR-GUV application in indoor settings [28] was used in the simulations. The commercial CFD software, Ansys Fluent v19.2, was used to solve the governing equations of the Realizable κ-ε turbulent model [36] with the SIMPLE algorithm. The software package states that this model offers certain advantages over the standard and possibly over the RNG κ-ε turbulent model [37], which is suitable for approximating turbulence due to buoyancy flows [38]. Boussinesq approximation was used to account for the buoyancy force on convective flows around the warm surfaces, such as light and body surfaces. The PRESTO! algorithm for pressure-velocity coupling was used, with the second-order upwind spatial discretization for momentum, κ, ε, and energy, and first-order upwind spatial discretization for scalar. The convergence criterion was 1×10^{-6} for energy, 1×10^{-15} for scalar, and 5×10^{-4} for other variables.

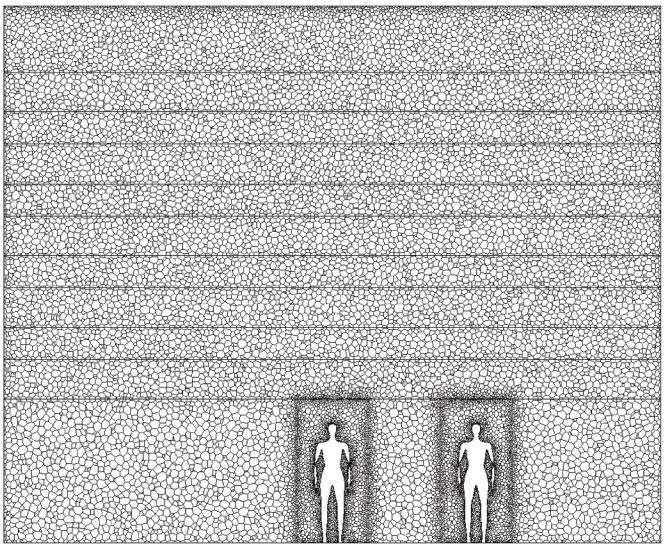

Fig. 2. Meshes in the sections across the standing human bodies in rehearsal room model.

After obtaining flow field, we simulated the spread of exhaled viruses following air currents, with the drift-flux model [39] using an active scalar to represent SARS-CoV-2. The governing equation is as follows:

$$\nabla \bullet \left(\left(\vec{V} + \overrightarrow{V_s} \right) C \right) = \nabla \bullet ((\lambda + \lambda_t) \nabla C) + S - zEC \quad (1)$$

where C is quanta concentration (quanta/m^3), $\vec{V}$ is the velocity vector of air (m/s), $\overrightarrow{V_s}$ is the setting velocity vector of quanta (m/s), λ and λ_t are laminar and turbulent diffusivity (m^2/s), S is the source term (quanta/m^3·s), z is the UV susceptibility constant [m^2/J], and E is the fluence rate [W/m^2]. $\overrightarrow{V_s}$ can be calculated using the aerosols' density and size with Stokes' law; therefore, it accounts for the gravitational force on the infectious aerosols, which were assumed to have an aerodynamic diameter of 5 μm. With Eq. (1), the influence of indoor humidity and temperature on aerosol size and the deposition of aerosols on the solid surfaces were ignored. In the simulations, z was set to be 0.2 m^2/J [40], and E was set to be 0.2 W/m^2, according to an estimate of 0.012 W/m^3 for the classroom's volume.

2.3. Boundary conditions

Table 1 summarizes the boundary conditions. For the bus models, the boundary conditions, including air temperatures for air supply and exhaled air, and surface temperatures for body sections, inner surfaces such as windows, windshield, floor, and lights, were derived from the data measured in our previous study on influenza transmission in buses [33]. In the classroom and rehearsal room models, boundary conditions

Table 1
Boundary conditions.

Boundary	Bus	Classroom	Rehearsal Room
Inlet	*V*: 1.06 m/s; *T*: 20.2°C	*V*: 5.59 m/s at horizontal direction, 3.23 m/s downward; *T*: 22 °C	*V*: 0.31 m/s; *T*: 22°C
Outlet	Free-slip	Free-slip	Free-slip
Lights	No-slip; *T*: 25.0°C		No-slip; *T*: 40.0°C
Ceiling	Adiabatic	Adiabatic	No-slip; *T*: 22.5°C
Floor	No-slip; *T*: 17.2°C	Adiabatic	No-slip; *T*: 21.0°C
Windows	No-slip; *T*: 16.8°C		
Walls	Adiabatic	Adiabatic	No-slip; *T*: 21.7°C
Human body	No-slip; *T*: varied in body sections [33]	No-slip; Convective heat release: 33.8 W	No-slip; Convective heat release: 33.8 W
Openings for breathing	*V*:1.07 m/s; *T*: 34°C for exhalation	*V*: 3.87 m/s for talking (teacher), 1.07 m/s for inhalation (student); *T*: 34°C for talking	*V*: 0.52 m/s for singing, 1.87 m/s for the standing ones' inhalation, 2.8 m/s for the seated one's inhalation; *T*: 34°C for singing
Other walls	Adiabatic	Adiabatic	Adiabatic

for inlet were given based on the air exchange rate of 3 ACH, and a convective heat flux of 33.8 W was uniformly given at the body surface [41]. We measured surface temperatures for the wall surfaces regarding its large indoor space. Breathing rate was given upon activity levels, 8 l/min for seated people (1.0 met), and 14 l/min for standing persons (1.8 met) [33,42]. Particularly, in the classroom model, when B (the teacher giving a lecture) was taken as the index case, the velocity at mouth opening was set as to be talking [43]; in the rehearsal room, when B was taken as the index case, the velocity was set at mouth opening as to be singing [44]. A quanta generation rate of 100 quanta/h was set at mouth/nose opening when one was taken as the index case [45]. Moreover, regarding air recirculation, the user-subroutines were created to get the average viral concentration at the outlet at the end of each step, calculate viral concentration of the supplied airflow based on mass balance according to air recirculation rate and the filter's particle removal efficiency (0.2 for MERV4, 0.7 for MERV 8, and 0.9 for MERV13), and set this concentration as the boundary condition at the inlets for the next step.

2.4. Evaluation of UV performance

Two traditional indices, i.e., fraction remaining (*FR*), and equivalent ventilation rate attributed to UV irradiation (λ_e) [46], were used to evaluate UV performance, calculated based on the viral concentration averaged with cell volumes as weighers (C_{ave}). *FR* can be calculated as the ratio of the C_{ave} values obtained with UV turned on and off, respectively. Then, λ_e can be calculated as follows:

$$\lambda_e = \frac{(1 - FR)}{FR}\lambda \tag{2}$$

where, λ is the ambient ventilate rate (ACH), i.e., the rate of air exchange by outdoor air or clean air.

In this study, we investigate the UR-GUV performance in the near field (NF) and far field (FF) from the index case. Here, we first defined breathing zone as the region between the heights of 1.1 m and 1.8 m above the floor, then took NF as the breathing zone within the distance of 0.9 m (3 ft) from the index case, and FF as the breathing zone outside of NF. Moreover, as λ is unknown in NF and FF in the cases with air recirculation, this study use (λ_e/λ) to evaluate the increase of ACH by using UR-GUV.

2.5. Evaluation of airborne infection risk

The infection risk caused by aerosol route can be evaluated with the viral concentration in the inhalation by the Well-Riley equation [47], as follows:

$$P = 1 - e^{-pCt} \tag{3}$$

where, *P* is the infection risk, *p* is the breathing rate (m^3/s), and *t* is the total exposure time that an occupant is exposed in the air mixed with the SARS-CoV-2 (s).

3. Results

We will introduce the results related to viral distribution and UV performance in the classroom, airport bus, and rehearsal room in turn. These results include (1) spatial distribution of viral concentrations, (2) C_{ave} in the whole room space (WR), NF and FF, (3) *FR* and (λ_e/λ) in WR, NF and FF; and (4) exposure time to reach 1% infection risk ($T_{1\%}$) in NF and FF. Particularly for the rehearsal room, we will also present the variations of C_{ave} with UV on, *FR* and (λ_e/λ), along with the elevation and height of UV zone.

3.1. Classroom model

Classroom represents a general application of UR-GUV with a typical ceiling height.

Viral Concentration Distribution. According to Fig. 3, independent of ventilation condition and source location, viral concentrations of 0.1 quanta/m^3 or greater cover a broad area throughout the room when UV is off. With UV on, high concentrations only exist in the vicinity of the index case. For the standing index case, the high concentrations only exist in the upper room behind the body.

C_{ave}, *FR* and (λ_e/λ). Fig. 4 compares C_{ave}, *FR*, and (λ_e/λ) for each scenario. Independent of body position, either with UV on or off, C_{ave} is almost same in WR and FF but much higher in NF in each case. The C_{ave} values in the LF case are much higher than the results in the CA and HF case with UV off, but similar to the results in the CA and HF case with UV on. Using UR-GUV can effectively reduce C_{ave} not only in FF but also in NF. As well as C_{ave}, independent of body position, *FR* is similar in WR and FF, but much higher in NF. *FR* values in the LF case are smaller than those in the CA and HF cases. Each *FR* for the seated index case is slightly higher than the corresponding *FR* for the standing index case. In contrast to *FR*, (λ_e/λ) in NF is less than 2, much smaller than those in WR and FF, which are greater than 8. (λ_e/λ) in FF is similar to that in WR for the seated index case, but obviously larger than that in WR for the standing index case.

$T_{1\%}$. Table 2 compares the $T_{1\%}$ for each scenario in the classroom model. According to the results in FF as given in Table 2, to limit

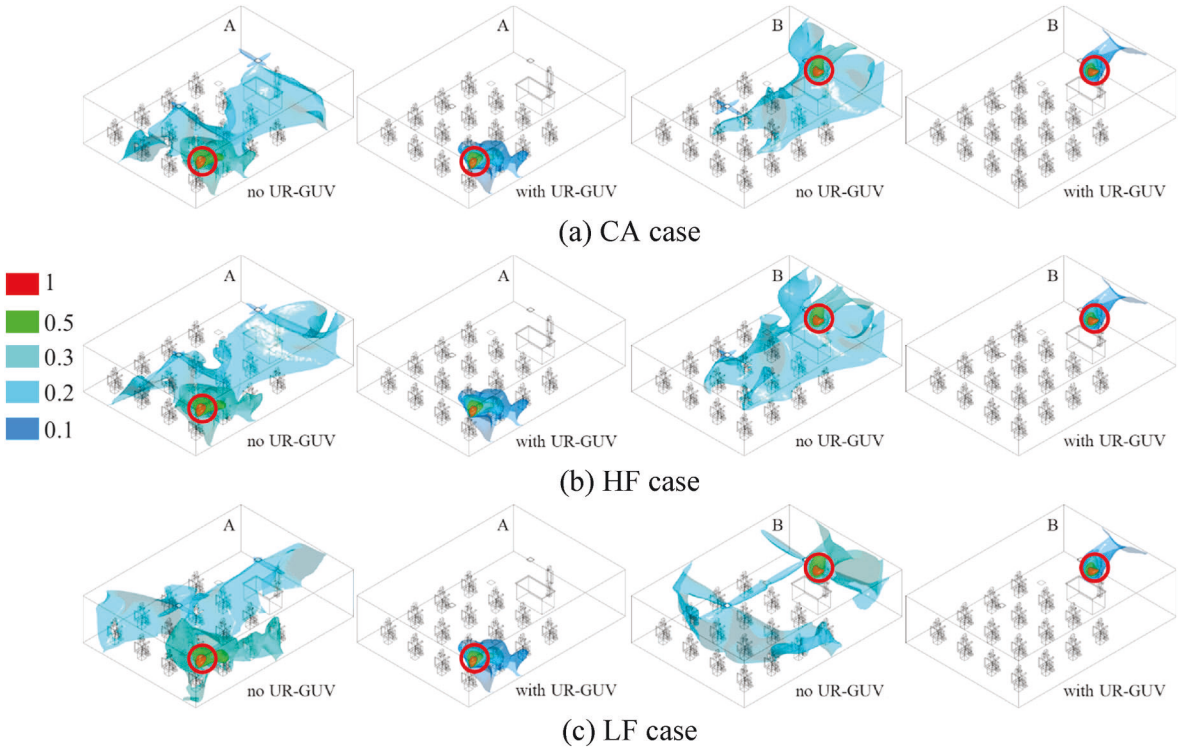

Fig. 3. Spread of viral bioaerosols from the index cases in the classroom, with UR-GUV turned on and off, respectively, demonstrated by concentration iso-surfaces in each case (quanta/m^3). Red circle highlights the index case. (For interpretation of the references to colour in this figure legend, the reader is referred to the Web version of this article.)

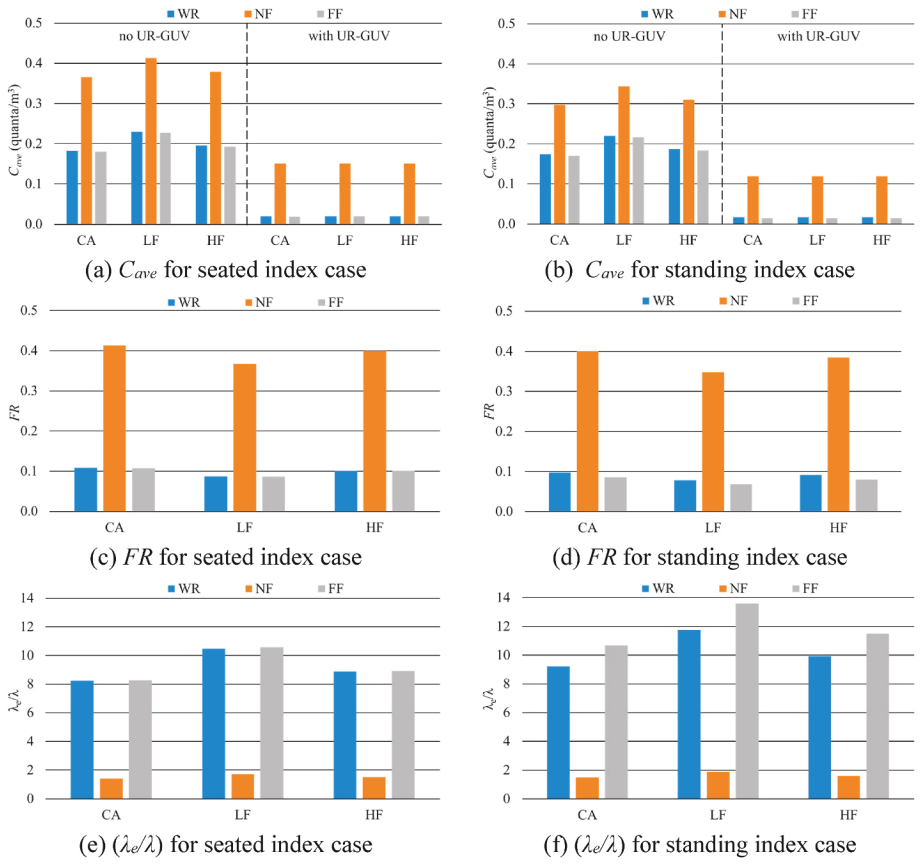

Fig. 4. Comparison of UR-GUV performance under different source and ventilation conditions in the classroom.

Table 2
Exposure time to reach 1% infection risk in NF and FF in the classroom, under different source, ventilation, and UR-GUV application conditions (Unit: min).

GUV use	No GUV			With GUV		
Case	CA	LF	HF	CA	LF	HF
Seated-NF	3.4	3.0	3.3	8.3	8.3	8.3
Standing-NF	4.2	3.6	4.0	10.5	10.5	10.5
Seated-FF	7.0	5.5	6.5	64.6	64.0	64.4
Standing-FF	7.4	5.8	6.8	86.0	84.5	85.5

infection risk under 1%, people can stay indoors no longer than 7 min with UV off in the CA case, but up to 64 min with the seated index case, and up to 84 min with the standing index case with UV on, even in the LF case. Apparently, using UV can ensure a safe lecture by following social distancing rule, in a classroom with a typical ceiling height for UR-GUV application.

3.2. Airport bus models

Airport bus represent indoor spaces with a low ceiling.

Viral Concentration Distribution. Fig. 5 demonstrates the spread of SARS-CoV-2 from the seated index case, for the two bus models. With UV turned off, we can see that the increased OR impedes the spread of viruses, concentrating viruses where around the index case. The low filtration in LF case caused the relatively higher viral concentration to be far away from the index case. With UV on, viral distribution was similar in the three cases. UV irradiation shows little influence on the virus concentrations around the index case. The results for the standing index case are not presented here because they are qualitatively similar outcome. Nevertheless, because the viruses from the standing index case are released closer to the ceiling, high viral concentrations are more distributed where close to the ceiling.

C_{ave}, FR and (λ_e/λ). Fig. 6 demonstrates the UR-GUV performance of 25% OR and 45% OR models in the airport bus. Qualitatively similar to the results of classroom, with the same conditions of OR and UR-GUV, C_{ave} is much higher in NF than in WR and FF, and C_{ave} in the LF case is higher than those in the CA and HF cases. However, quantitively apparently, C_{ave} values are much higher than those corresponding values (with the same conditions of UR-GUV, ventilation, and spatial relationship to source) in the classroom, especially with a seated index case. Moreover, with the same index case, C_{ave} with the 25% OR model is a little higher in WR and FF, but much lower in NF when compared to the results with 45% OR model. Remarkably, with 45% OR, the NF C_{ave} values for the standing index case are much lower than those for the seated index case.

FR is greatest in NF and lowest in FF, with the same conditions of UR-GUV, OR, ventilation and body position. *FR* values are higher for the seated index case than the corresponding values for the standing index case, especially with 45% OR. As well as C_{ave}, *FR* values are always higher in the bus models than the relative values in the classroom model. Particularly, in the CA case with the seated index case and 45% OR, *FR* in WR is 8 times that in the classroom. The results of (λ_e/λ) are qualitatively contrary to the results of *FR*. Remarkably, (λ_e/λ) values are lower than 1.3 for the seated index case and lower than 2 for the standing index case.

$T_{1\%}$. Table 3 compares the $T_{1\%}$ for each scenario in the airport bus models. With 25% OR, people can only stay 6.2 min in FF in the LF case, but 11.3 min in the CA case, when UR-GUV is off. When using UR-GUV, people cannot stay longer than 5.4 min in NF, but stay in FF at least 14.1 min with 25% OR and 16.1 min with 45% OR. With the same OR, $T_{1\%}$ can be extended with high filtration, and further extended a little with 100% clean air supply regardless of the use of UR-GUV. Moreover, we can see that $T_{1\%}$ increases along with OR, and people can stay longer in the airport bus with the standing index case. Compared to the results with the classroom model, using UR-GUV in the airport bus cannot significantly prolong the staying time in FF as in the classroom.

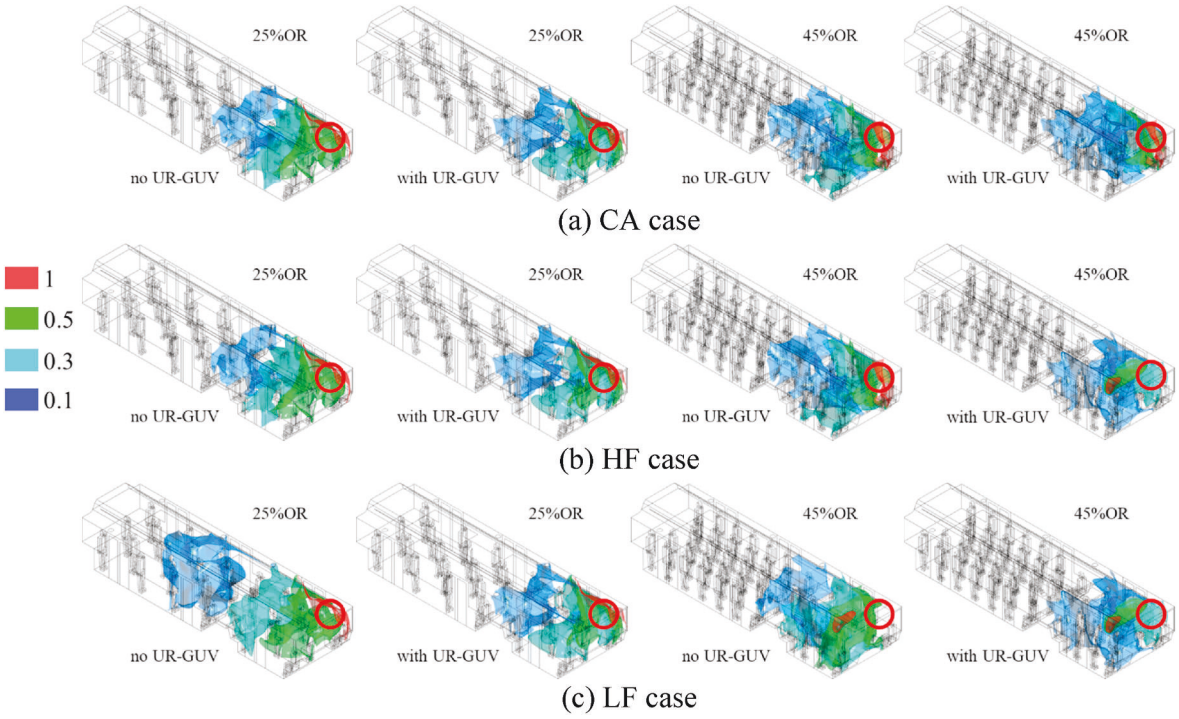

Fig. 5. Spread of viral bioaerosols from the seated index case (A) in the airport bus, with UR-GUV turned on and off, demonstrated by concentration iso-surfaces in each case (quanta/m^3). Red circle highlights the index case. (For interpretation of the references to colour in this figure legend, the reader is referred to the Web version of this article.)

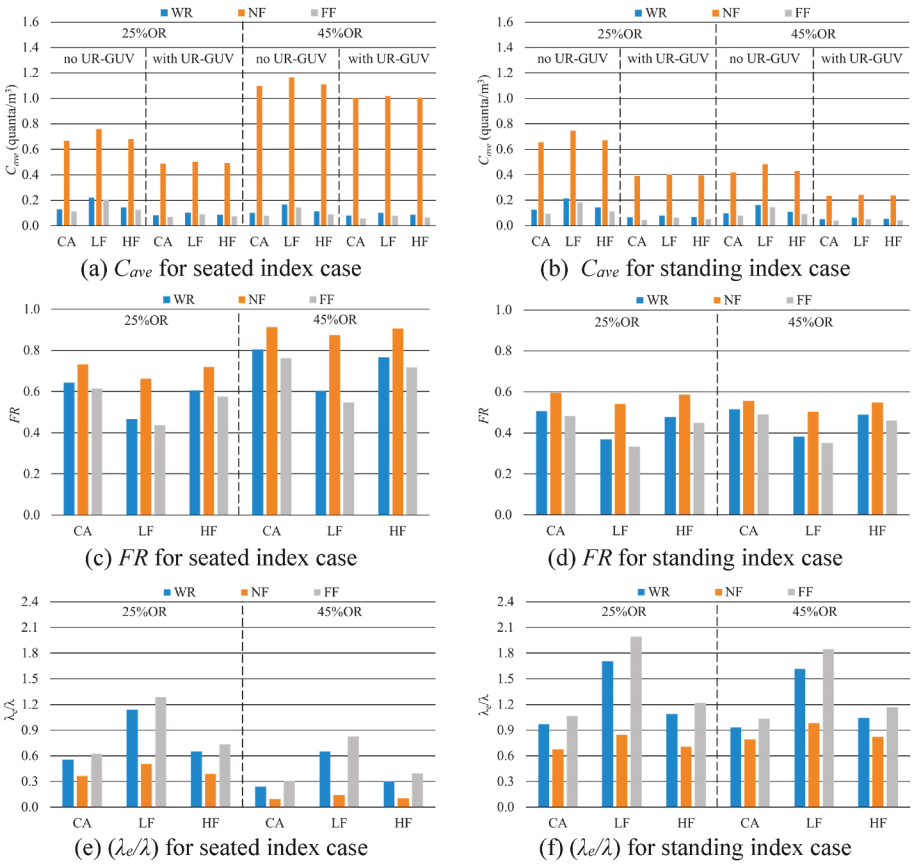

Fig. 6. Comparison of UR-GUV performance under different source, OR, and ventilation conditions in the airport bus.

Table 3
Exposure time to reach 1% infection risk in NF and FF in the airport bus, under different source, ventilation, and UR-GUV application conditions (Unit: min).

GUV use	No GUV						With GUV					
Case	CA		LF		HF		CA		LF		HF	
OR	25%	45%	25%	45%	25%	45%	25%	45%	25%	45%	25%	45%
Seated-NF	1.9	1.1	1.7	1.1	1.8	1.1	2.6	1.3	2.5	1.2	2.6	1.2
Standing-NF	1.9	3.0	1.7	2.6	1.9	2.9	3.2	5.4	3.1	5.1	3.2	5.3
Seated-FF	11.3	16.4	6.2	8.8	9.8	14.2	18.3	21.4	14.1	16.1	17.1	19.8
Standing-FF	13.4	15.8	6.9	8.7	11.5	13.8	27.8	32.2	20.6	24.7	25.5	29.9

3.3. Rehearsal room model

The rehearsal room has an extremely high ceiling. This section will first investigate the influences of UV zone's elevation and height on UV air disinfection efficacy, then present the results with the UV zone between 2 m and 4 m.

3.3.1. Influence of UV zone elevation

We assumed a UV zone with a height of 1 m, then repeated the scalar transport simulation with the UV zone started from 2 m, 3 m, 4 m, 5 m, and 6 m, with the 100% clean air supply (CA case). The variations of C_{ave} with UV on, *FR* and (λ_e/λ) in WR, NF and FF are summarized in Table 4. Apparently, UV zone elevation is not a key parameter to the UR-GUV's disinfection efficacy even under an imperfect air mixing condition.

Table 4
Variations of UR-GUV performance with UV zone elevation (mean ± std.).

Index case	Region	C_{ave} (quanta/m^3)	*FR*	λ_e/λ
A (seated)	WR	0.0111 ± 0.0008	0.157 ± 0.011	5.4 ± 0.5
	FF	0.0125 ± 0.0011	0.172 ± 0.015	4.9 ± 0.5
	NF	0.0210 ± 0.0012	0.253 ± 0.014	3.0 ± 0.2
B (Standing)	WR	0.0094 ± 0.0003	0.141 ± 0.004	6.1 ± 0.2
	FF	0.0092 ± 0.0004	0.137 ± 0.007	6.3 ± 0.3
	NF	0.0316 ± 0.0006	0.352 ± 0.007	1.8 ± 0.1

3.3.2. Influence of UV zone height

With 100% clean air supply (CA case) condition, we repeated the scalar transport simulation with the UV zone height varying from 1 m to 5.47 m. All of the UV zones started at the elevation of 2 m. Fig. 7 presents the changes of C_{ave} with UV on, *FR* and (λ_e/λ) along with the increase of UV zone height, for the seated and standing index case, respectively. We can see that all three parameters have power relationships with UV zone height. C_{ave} and *FR* decrease with UV zone height with similar trends, but have much greater values in NF than in WR and FF. In contrast, (λ_e/λ) increases with UV zone height and increases much faster in WR and FF than in NF. Particularly, with the standing index case, when UV zone height increases from 1 m to 5.47 m, (λ_e/λ) increases 28.4 in WR and 30.4 in FF, but only 0.8 in NF.

3.3.3. Results with UV zone height between 2 m and 4 m

Viral Concentration Distribution. According to Fig. 8, the viral

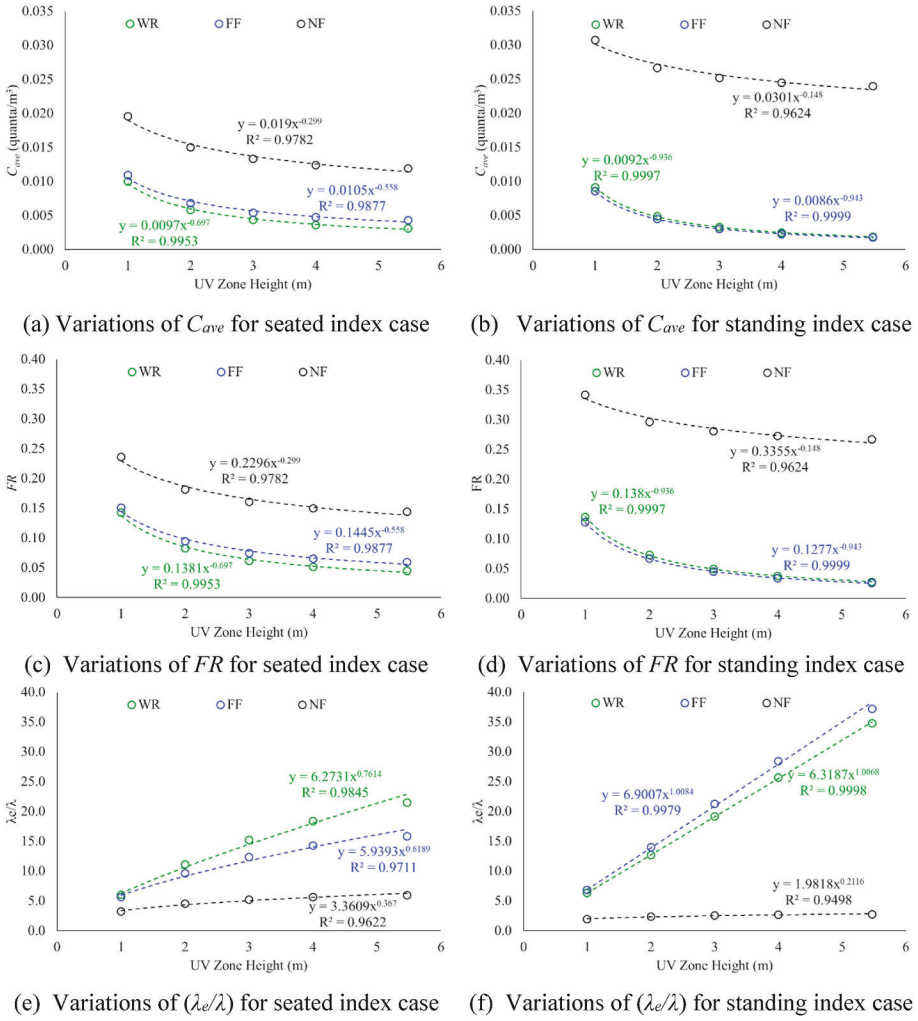

(a) Variations of C_{ave} for seated index case (b) Variations of C_{ave} for standing index case

(c) Variations of FR for seated index case (d) Variations of FR for standing index case

(e) Variations of (λ_e/λ) for seated index case (f) Variations of (λ_e/λ) for standing index case

Fig. 7. Influence of UV zone height on UR-GUV performance in the CA case in the rehearsal room.

concentrations of ≥0.1 quanta/m^3 cannot cover the mouths/noses of the recipients in the CA and HF cases when UV is off. Using UR-GUV makes the distributions of viral concentrations of ≥0.1 quanta/m^3 limited in a very small area around the index case, even in the LF cases, diminishing the differences in the viral distribution under each ventilation condition.

C_{ave}, FR and (λ_e/λ). According to Fig. 9, C_{ave} values are much smaller than the corresponding values obtained with the bus and classroom models, as well as the differences caused by UR-GUV use and by body position. Importantly, using UR-GUV also significantly reduces C_{ave} in NF; however, C_{ave} in NF is still much greater than C_{ave} in WR and FF.

FR values in the rehearsal room are relatively smaller than the corresponding results in the classroom. FR is much higher in NF than in WR and FF in each case. As well as in other models, the results for (λ_e/λ) are qualitatively opposite to the results of FR. Moreover, (λ_e/λ) results in the rehearsal room are higher than the corresponding results in the classroom.

$T_{1\%}$. Table 5 compares the $T_{1\%}$ for each scenario in the rehearsal model. According to the results in FF as given in Table 5, without using UR-GUV, the music class can only continue up to 17.3 min even in the CA case. If using UR-GUV, music class can be extended to over 182 min, around 3 times that in the classroom, fully ensuring the requirement of music classes.

4. Discussion

4.1. Rationality of simulation results

There have been countless studies on UR-GUV performance; however, these studies varied in the parameters, such as room configuration, ventilation, microorganism, UR-GUV system and the resulted UV zone. As a whole-room air disinfection method, UR-GUV has never been investigated in NF and FF; and it is not easy to theoretically estimate UR-GUV performance in NF and FF. Accordingly, this discuss on the rationality of simulation results will be focused on the FR values of the whole room, based on the comparison to the theoretic estimation of FR based on perfect mixing assumption.

For a perfectly mixed room, the average FR of the whole room in the CA case can be calculated with the following equation [28]:

$$FR = \frac{1}{1 + z\bar{E}\tau_n} \tag{4}$$

where, $\bar{E}$ is the average fluence rate in the room [W/m^2], and τ_n is the nominal time constant [s], which is the inverse of air exchange rate. With Eq. (4), we calculated the FR values as summarized in Table 6.

According to the simulation results of the classroom and rehearsal room models, indoor average viral concentration varies little with the source location, which is around 5% with UV off and 15% with UV on. Furthermore, as illustrated in Figs. 4 and 9, FR is similar in FF and WR in the two room models. These results indicate a pretty good air mixing in

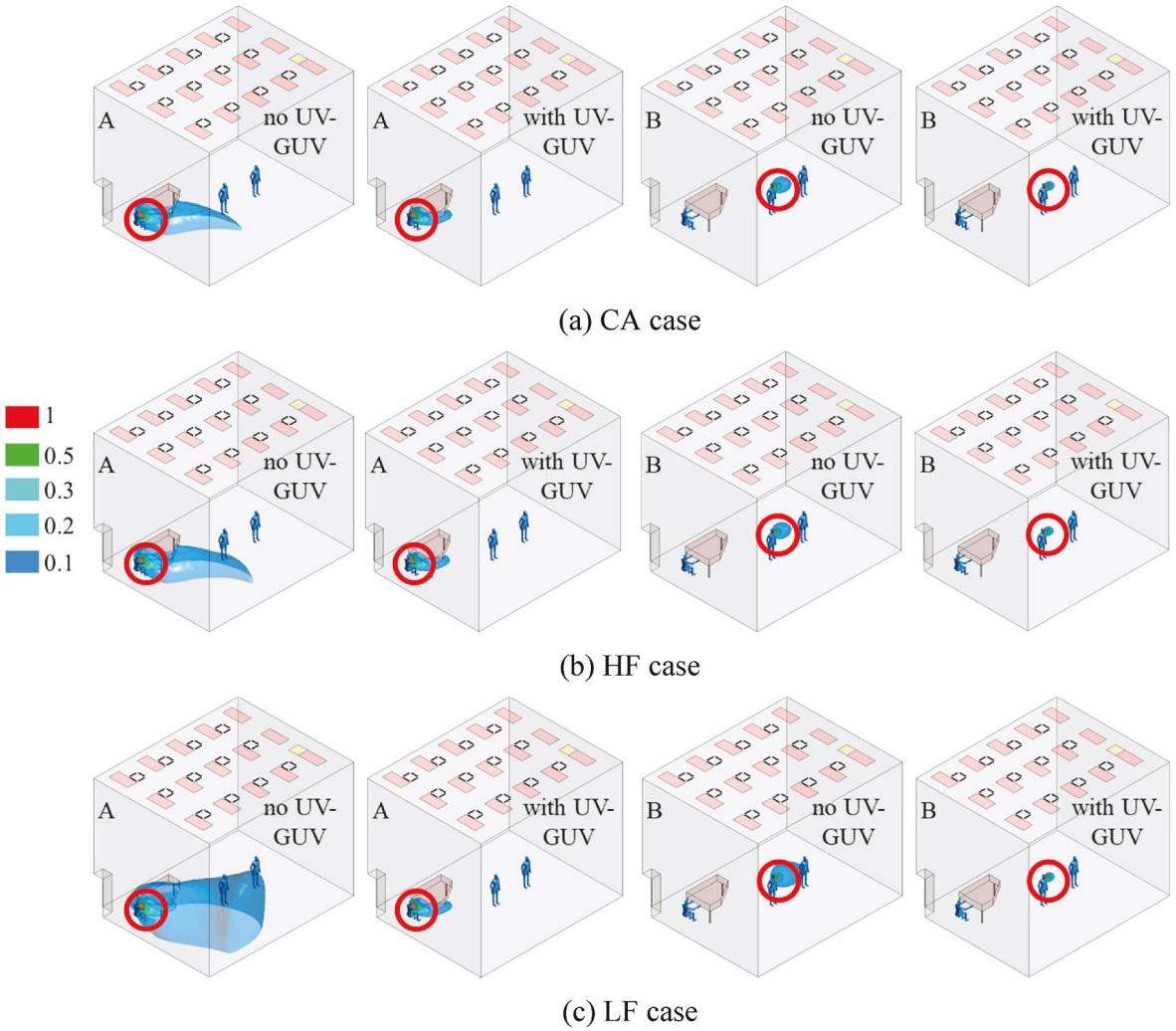

Fig. 8. Spread of viral bioaerosols from the index cases in the rehearsal room, with UR-GUV turned on and off, respectively, demonstrated by concentration iso-surfaces in each case (quanta/m^3). Red circle highlights the index case. (For interpretation of the references to colour in this figure legend, the reader is referred to the Web version of this article.)

the two rooms. As a result, as shown in Table 6, the CFD results are greater but very close to their corresponding theoretic *FR* value in the two rooms. To the opposite, we can see that the CFD results deviate significantly from their corresponding theoretic *FR* value in the airport bus, especially with a higher OR, due to the poor air mixing. Accordingly, we consider the simulation results are rational and acceptable.

4.2. UR-GUV's air disinfection effect and impact of ceiling

Apparently, UR-GUV using 254 nm UV light is an advantageous non-pharmaceutical intervention (NPI) measure for preventing the spread of COVID-19 virus transmission for an indoor setting such as classroom. Consistent with previous studies, the traditional UR-GUV application in the classroom can effectively reduce indoor viral concentration for COVID-19 [48–50]. As a result, it provides sufficient air disinfection effect with the overall aerosol infection risk of COVID-19 down to an acceptable level. However, it can only reduce viral concentration by up to 65% in NF in the classroom. This whole-room NPI is incapable for local air disinfection around human bodies even there is a good air mixing. To accomplish a lecture with an infection risk lower than 1%, it is essential to keep a 6-ft social distance between the occupants.

On the contrary, UR-GUV with 254-nm UV light indicates not a promising air disinfection measure for an indoor setting such as airport bus. Obviously, ceiling height and configuration limited the space for UV irradiation and air mixing in the airport bus. The UV zone had to be placed in the concave-upward space in the middle of the airport bus, where had a relatively high ceiling of 2.45 m. As a result, the UV zone's volume is 6.5 m^3 in the airport bus, only around 14.5% of that in the classroom, which is 44.8 m^3. A recent study particularly pointed that UV zone volume has a notable effect on UR-GUV performance, and is more critical than UV fluence rate [35]. Meanwhile, although air exchange rate in the airport bus is 10 times that in the classroom and rehearsal room, viral concentration is much higher in NF regardless whether UR-GUV is used or not, and even much higher in FF when using UR-GUV. This is because the existence of passengers impedes air mixing in both vertical and horizontal directions. Many studies have emphasized that air mixing, especially vertical air mixing, is crucial for UR-GUV performance in air disinfection [26,51–54]. Although using UR-GUV can keep infection risk lower than 1% in FF for around 14 min in the airport bus; in practice, it is difficult to follow social distancing in the airport bus, meanwhile no one can ensure himself/herself in the FF regarding the vast number of asymptomatic COVID-19 patients [55]. Therefore, it is necessary and important to use personal protection equipment, such as a mask to prevent infection transmission in the airport bus even with UV on. A meta-analysis shows that wearing any kind of face masks can significantly reduce the infection risk for COVID-19 [56]. Mask-wearing can reduce the risk of COVID-19 infection by 81% [57]. Another effective measure is to effectively clean air in

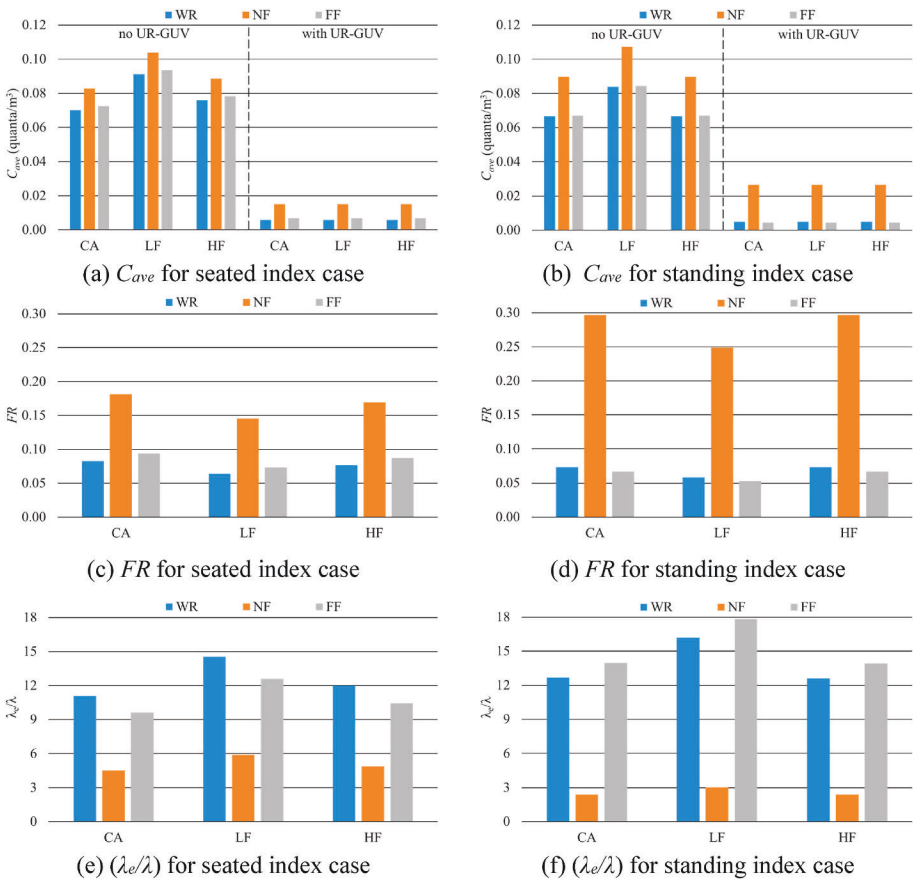

Fig. 9. Comparison of UR-GUV performance under different source and ventilation conditions in the rehearsal room.

Table 5
Exposure time to reach 1% infection risk in NF and FF in the rehearsal room, under different source, ventilation, and UR-GUV application conditions (Unit: min).

GUV use	No GUV			With GUV		
Case	CA	LF	HF	CA	LF	HF
Seated-NF	15.2	12.1	14.2	83.5	83.3	83.5
Standing-NF	14.0	11.7	14.0	47.2	47.1	47.1
Seated-FF	17.3	13.4	16.1	184.1	182.8	183.6
Standing-FF	18.8	14.9	18.8	281.0	280.3	280.0

Table 6
Comparison of *FR* under perfect mixing condition to the calculated values.

Model	*FR*		
	Perfect mixing	CFD/Seated index case	CFD/Standing index case
Classroom	0.093	0.108	0.098
Rehearsal room	0.072	0.083	0.073
Airport bus with 25% OR	0.179	0.643	0.507
Airport bus with 45% OR	0.176	0.805	0.517

NF. One promising option is to use the far UV light with a wavelength of 222 nm, which is able to distribute safe UV irradiation in the breathing zone to efficiently clean exhaled air [58]. Because 222 nm light can greatly increase the safety threshold limit values for UV exposure [59], it is particularly suitable for airport buses with a relatively short travel.

Exactly the opposite to airport bus, the rehearsal room with such a high ceiling affords more spaces for UV irradiation and air mixing. UR-GUV can reduce viral concentration in NF by over 70% with a seated source and by over 81% with a standing source. As a result, the occupants can stay 47 min even in NF. Moreover, the slightly different UV performance with the two index cases indicates that there is still room to improve UR-GUV performance in NF by using ceiling fans to promote indoor air mixing [28]. Conceivably, with ideal perfect air mixing, the UV dose, as well as UV disinfection efficacy will be completely independent of UV zone elevation. Importantly, the high ceiling allows to move the UV zone to a high elevation and enable the use of an open fixture without louvers to generate the UV zone with high UV irradiation; moreover, it also enables to increase the volume for UV zone, which has been proved to more effective to improve UR-GUV performance than increasing UV fluence rate [35]. In conclusion, high ceiling makes UR-GUV a more powerful NPI measure against indoor air disinfection, not only effective in FF, but also in NF.

4.3. Limit of high filtration and impact of UR-GUV

Certainly, upgrading to the high-level filtration can effectively reduce viral concentration in the bus and classroom and rehearsal room, not only in FF, but also in NF, achieving the effect comparable to supplying 100% clean air. But obviously, the effect of high-level filters is limited. Moreover, even 100% clean air cannot significantly reduce viral concentration, satisfying the recommendations for aerosol infection control. More importantly, SARS-CoV-2 virions range between 0.06 and 0.14 μm in diameter [60], and most of exhaled aerosols are smaller than 4 μm with a median between 0.7 and 1.0 μm [61]. And according to ASHRAE standard 52.2 [19], even a MERV13 filter can only remove 50% of particle between 0.3–1.0 μm at largest; therefore, the effects of these filters on COVID-19 viral concentration and infection risk are

overestimated in the simulations. As a result, with the ventilation and occupancy conditions given in this study, the HVAC system with high-level filters (even HEPA filters) cannot provide safe environments.

Our simulations also show that UR-GUV has a persistent better performance in the LF case than in the CA and HF case. In the LF case, using UR-GUV reduced the viral concentration to the similar level obtained with 100% clean air supply, both in FF and NF, even in the airport bus. Potentially there is a huge energy saving for indoor aerosol infection control because compared to the energy used for cooling or heating 100% outdoor air supply or pushing air through HEPA filters with high resistance, UR-GUV can be an economic option. With a rough estimation, it may be able to save approximately 19.4% annual energy consumption for the rehearsal room by using the LF air recirculation/filtration condition, if the building is located in the College Park, MD area.

4.4. Limits of the present study

This study investigated efficacy of UR-GUV with a uniform fluence rate distribution in the UV zone, which is an assumption representing the upper limit for the lamp performance. A follow-up study will improve the quantitative prediction for UR-GUV disinfection efficacy with UV fluence rate distribution to be created with a computer-aided design (CAD) software. Based on the spatial distribution of UV disinfection efficacy, it will be possible to optimize efficient UR-GUV design with the consideration of UV energy consumption.

5. Conclusions

This study investigated UR-GUV disinfection efficacy in the NF and FF in three indoor settings with low ceiling (airport bus), medium ceiling (classroom), and high ceiling (rehearsal room). Ceiling height and configuration is a crucial factor to UR-GUV performance because it determines the space volume available for air mixing and UV irradiation. UR-GUV cannot provide sufficient safety for environments with low ceiling, such as airport bus, so mask-wearing is recommended for the occupants. Keeping social distancing is recommended for classroom and rehearsal room even when using UR-GUV because UR-GUV cannot sufficiently reduce infection risk in NF. It is possible to further improve UR-GUV performance in NF by promoting air mixing in the two rooms. In spaces with high ceilings, UV disinfection efficacy follows power relationship with UV zone height, so the UV disinfection efficacy has a power relationship with the UV dose. Overall, when using UR-GUV, it is no longer necessary to upgrade filtration or use 100% outdoor air for indoor infection control.

CRediT authorship contribution statement

Shengwei Zhu: Writing – review & editing, Writing – original draft, Visualization, Methodology, Investigation, Funding acquisition, Conceptualization. **Tong Lin:** Methodology. **Lingzhe Wang:** Methodology. **Edward A. Nardell:** Writing – review & editing, Resources, Methodology. **Richard L. Vincent:** Writing – review & editing, Resources, Methodology. **Jelena Srebric:** Writing – review & editing, Supervision, Resources, Project administration, Methodology, Investigation, Funding acquisition, Conceptualization.

Declaration of competing interest

The authors declare the following financial interests/personal relationships which may be considered as potential competing interests: Jelena Srebric reports financial support was provided by National Science Foundation.

Data availability

No data was used for the research described in the article.

Acknowledgement

This study was sponsored by the RAPID-ES project “Energy-Efficient Disinfection of Viral Bioaerosols in Public Spaces: Vital for Lifting of the “Stay-at-Home” Orders during the Covid-19 Outbreak” by National Science Foundation (NSF) (Award number: 2032107).

References

[1] World Health Organization, Infection Prevention and Control of Epidemic-And Pandemic Prone Acute Respiratory Infections in Health Care, 2014. https://www.who.int/publications-detail-redirect/infection-prevention-and-control-of-epidemic-and-pandemic-prone-acute-respiratory-infections-in-health-care. (Accessed 11 November 2021).

[2] W. Chen, N. Zhang, J. Wei, H.-L. Yen, Y. Li, Short-range airborne route dominates exposure of respiratory infection during close contact, Build. Environ. 176 (2020), 106859, https://doi.org/10.1016/j.buildenv.2020.106859.

[3] G. Scheuch, Breathing is enough: for the spread of influenza virus and SARS-CoV-2 by breathing only, J. Aerosol Med. Pulm. Drug Deliv. 33 (2020) 230–234, https://doi.org/10.1089/jamp.2020.1616.

[4] V. Stadnytskyi, C.E. Bax, A. Bax, P. Anfinrud, The airborne lifetime of small speech droplets and their potential importance in SARS-CoV-2 transmission, Proc. Natl. Acad. Sci. USA 117 (2020) 11875–11877, https://doi.org/10.1073/pnas.2006874117.

[5] J.W. Tang, L.C. Marr, Y. Li, S.J. Dancer, Covid-19 has redefined airborne transmission, BMJ (2021) n913, https://doi.org/10.1136/bmj.n913.

[6] CDC, Guidelines for Preventing the Transmission of Mycobacterium tuberculosis in Health-Care Facilities, Centers for Disease Control and Prevention, 1994. https://www.cdc.gov/mmwr/preview/mmwrhtml/00035909.htm. (Accessed 12 November 2021), 1994.

[7] A. James, L. Eagle, C. Phillips, D.S. Hedges, C. Bodenhamer, R. Brown, J. G. Wheeler, H. Kirking, High COVID-19 attack rate among attendees at events at a church - Arkansas, March 2020, MMWR Morb. Mortal. Wkly. Rep. 69 (2020) 632–635, https://doi.org/10.15585/mmwr.mm6920e2.

[8] D.C. Adam, P. Wu, J.Y. Wong, E.H.Y. Lau, T.K. Tsang, S. Cauchemez, G.M. Leung, B.J. Cowling, Clustering and superspreading potential of SARS-CoV-2 infections in Hong Kong, Nat. Med. 26 (2020) 1714–1719, https://doi.org/10.1038/s41591-020-1092-0.

[9] Y. Furuse, E. Sando, N. Tsuchiya, R. Miyahara, I. Yasuda, Y.K. Ko, M. Saito, K. Morimoto, T. Imamura, Y. Shobugawa, S. Nagata, K. Jindai, T. Imamura, T. Sunagawa, M. Suzuki, H. Nishiura, H. Oshitani, Clusters of coronavirus disease in communities, Japan, January-april 2020, Emerg. Infect. Dis. 26 (2020), https://doi.org/10.3201/eid2609.202272.

[10] Y. Li, H. Qian, J. Hang, X. Chen, P. Cheng, H. Ling, S. Wang, P. Liang, J. Li, S. Xiao, J. Wei, L. Liu, B.J. Cowling, M. Kang, Probable airborne transmission of SARS-CoV-2 in a poorly ventilated restaurant, Build. Environ. (2021), 107788, https://doi.org/10.1016/j.buildenv.2021.107788.

[11] Y. Shen, C. Li, H. Dong, Z. Wang, L. Martinez, Z. Sun, A. Handel, Z. Chen, E. Chen, M.H. Ebell, F. Wang, B. Yi, H. Wang, X. Wang, A. Wang, B. Chen, Y. Qi, L. Liang, Y. Li, F. Ling, J. Chen, G. Xu, Community Outbreak investigation of SARS-CoV-2 transmission among bus riders in Eastern China, JAMA Intern. Med. (2020), https://doi.org/10.1001/jamainternmed.2020.5225.

[12] Z. Zhang, T. Han, K.H. Yoo, J. Capecelatro, A.L. Boehman, K. Maki, Disease transmission through expiratory aerosols on an urban bus, Phys. Fluids 33 (2021), 015116, https://doi.org/10.1063/5.0037452.

[13] D.A. Christopherson, W.C. Yao, M. Lu, R. Vijayakumar, A.R. Sedaghat, High-efficiency particulate air filters in the era of COVID-19: function and efficacy, Otolaryngol. Neck Surg. 163 (2020) 1153–1155, https://doi.org/10.1177/0194599820941838.

[14] L.J. Schoen, Guidance for building operations during the COVID-19 pandemic, ASHRAE J. May 2020 (2020) 72–74.

[15] Updated air filtration systems, MICA, n.d. https://www.mica.edu/mica-dna/r5/fall-2021-reopening/revised-and-expanded-operational-mode-4/updated-air-filtration-systems/. (Accessed 27 November 2021).

[16] Update on HCPSS Measures for Enhancing Air Quality in School Buildings, HCPSS News, August 26, 2021 (n.d.), https://news.hcpss.org/news-posts/2021/08/update-on-hcpss-measures-for-enhancing-air-quality-in-school-buildings/. (Accessed 27 November 2021).

[17] B. Simms, Baltimore Updates Air Filters inside Older Buildings as COVID-19 Precautions, WBAL, 2020. https://www.wbaltv.com/article/baltimore-city-updates-air-filters-inside-older-buildings-coronavirus/34331341. (Accessed 27 November 2021).

[18] How Metro Improves Air Quality in Buses for Drivers and Passengers, Metro Matters, 2020. https://kingcountymetro.blog/2020/04/10/how-metro-improves-air-quality-in-buses-for-drivers-and-passengers/. (Accessed 27 November 2021).

[19] ANSI/ASHRAE Standard 52.2-2017 Method of Testing General Ventilation AIr-Cleaning Devices for Removal Efficiency by Particle Size, American Society of Heating, Refrigerating and Air-Conditioning Engineers, Atlanta, GA, 2017.

[20] W.F. Wells, M.W. Wells, T.S. Wilder, The environmental control of epidemic contagion: I. AN epidemiologic study of radiant disinfection of air in day schools, Am. J. Epidemiol. 35 (1942) 97–121, https://doi.org/10.1093/oxfordjournals.aje.a118789.

[21] G. Volchenkov, Experience with UV-C air disinfection in some Russian hospitals, Photochem. Photobiol. 97 (2021) 549–551, https://doi.org/10.1111/php.13418.

[22] CDC, Upper-room ultraviolet germicidal irradiation (UVGI), Cent. Dis. Control Prev (2020). https://www.cdc.gov/coronavirus/2019-nCoV/index.html. (Accessed 14 December 2021).

[23] L. Morawska, J.W. Tang, W. Bahnfleth, P.M. Bluyssen, A. Boerstra, G. Buonanno, J. Cao, S. Dancer, A. Floto, F. Franchimon, C. Haworth, J. Hogeling, C. Isaxon, J. L. Jimenez, J. Kurnitski, Y. Li, M. Loomans, G. Marks, L.C. Marr, L. Mazzarella, A. K. Melikov, S. Miller, D.K. Milton, W. Nazaroff, P.V. Nielsen, C. Noakes, J. Peccia, X. Querol, C. Sekhar, O. Seppänen, S. Tanabe, R. Tellier, K.W. Tham, P. Wargocki, A. Wierzbicka, M. Yao, How can airborne transmission of COVID-19 indoors be minimised? Environ. Int. 142 (2020), 105832 https://doi.org/10.1016/j.envint.2020.105832.

[24] M.W. First, R.A. Weker, S. Yasui, E.A. Nardell, Monitoring human exposures to upper-room germicidal ultraviolet irradiation, J. Occup. Environ. Hyg. 2 (2005) 285–292, https://doi.org/10.1080/15459620590952224.

[25] Environmental Control for Tuberculosis: Basic Upper-Room Ultraviolet Germicidal Irradiation Guidelines for Healthcare Settings, U.S. Department of Health and Human Services, Public Health Service, Centers for Disease Control and Prevention, National Institute for Occupational Safety and Health, 2009, https://doi.org/10.26616/NIOSHPUB2009105.

[26] S. Zhu, J. Srebric, S.N. Rudnick, R.L. Vincent, E.A. Nardell, Numerical investigation of upper-room UVGI disinfection efficacy in an environmental chamber with a ceiling fan, Photochem. Photobiol. 89 (2013) 782–791, https://doi.org/10.1111/php.12039.

[27] S. Zhu, J. Srebric, S.N. Rudnick, R.L. Vincent, E.A. Nardell, Numerical modeling of indoor environment with a ceiling fan and an upper-room ultraviolet germicidal irradiation system, Build. Environ. 72 (2014) 116–124, https://doi.org/10.1016/j.buildenv.2013.10.019.

[28] G. Pichurov, J. Srebric, S. Zhu, R.L. Vincent, P.W. Brickner, S.N. Rudnick, A validated numerical investigation of the ceiling fan's role in the upper-room UVGI efficacy, Build. Environ. 86 (2015) 109–119, https://doi.org/10.1016/j.buildenv.2014.12.021.

[29] J. Frantsve-Hawley, H.G.R. Jr, The mask ask: understanding and addressing mask resistance, J. Mich. Dent. Assoc. (2020) 38–44.

[30] S. Hills, Y. Eraso, Factors associated with non-adherence to social distancing rules during the COVID-19 pandemic: a logistic regression analysis, BMC Publ. Health 21 (2021) 352, https://doi.org/10.1186/s12889-021-10379-7.

[31] S. Zhu, T. Lin, J.G.C. Laurent, J.D. Spengler, J. Srebric, Tradeoffs between ventilation, air mixing, and passenger density for the airborne transmission risk in airport transportation vehicles, Build. Environ. 219 (2022), 109186, https://doi.org/10.1016/j.buildenv.2022.109186.

[32] M. Sandberg, M. Sjöberg, The use of moments for assessing air quality in ventilated rooms, Build. Environ. 18 (1983) 181–197, https://doi.org/10.1016/0360-1323(83)90026-4.

[33] S. Zhu, J. Srebric, J.D. Spengler, P. Demokritou, An advanced numerical model for the assessment of airborne transmission of influenza in bus microenvironments, Build. Environ. 47 (2012) 67–75, https://doi.org/10.1016/j.buildenv.2011.05.003.

[34] B. Pirouz, S.A. Palermo, S.N. Naghib, D. Mazzeo, M. Turco, P. Piro, The role of HVAC design and windows on the indoor airflow pattern and ACH, Sustainability 13 (2021) 7931, https://doi.org/10.3390/su13147931.

[35] S. Park, R. Mistrick, D. Rim, Performance of upper-room ultraviolet germicidal irradiation (UVGI) system in learning environments: effects of ventilation rate, UV fluence rate, and UV radiating volume, Sustain. Cities Soc. 85 (2022), 104048, https://doi.org/10.1016/j.scs.2022.104048.

[36] T.H. Shih, W. Liou, A. Shabbir, Z. Yang, J. Zhu, A new k-ε eddy viscosity model for high Reynolds number turbulent flows - model development and validation, Comput. Fluids 24 (1994).

[37] Ansys Fluent V19.2, ANSYS Fluent Theory Guide, 2018.

[38] Z.J. Zhai, Z. Zhang, W. Zhang, Q.Y. Chen, Evaluation of various turbulence models in predicting airflow and turbulence in enclosed environments by CFD: Part 1—summary of prevalent turbulence models, HVAC R Res. 13 (2007) 853–870, https://doi.org/10.1080/10789669.2007.10391459.

[39] S. Holmberg, Y. Li, Modelling of the indoor environment – particle dispersion and deposition, Indoor Air 8 (1998) 113–122, https://doi.org/10.1111/j.1600-0668.1998.t01-2-00006.x.

[40] N.C. Rockey, J.B. Henderson, K. Chin, L. Raskin, K.R. Wigginton, Predictive modeling of virus inactivation by UV, Environ. Sci. Technol. 55 (2021) 3322–3332, https://doi.org/10.1021/acs.est.0c07814.

[41] S. Zhu, S. Kato, J.-H. Yang, Study on transport characteristics of saliva droplets produced by coughing in a calm indoor environment, Build. Environ. 41 (2006) 1691–1702, https://doi.org/10.1016/j.buildenv.2005.06.024.

[42] Y. Nishi, Human and thermal environment, in: Mech. Comf. Therm. Environ, first ed., The Society of Heating, Air-Conditioning and Sanitary Engineers of Japan, Tokyo, Japan, 2005, p. 30.

[43] C.Y.H. Chao, M.P. Wan, L. Morawska, G.R. Johnson, Z.D. Ristovski, M. Hargreaves, K. Mengersen, S. Corbett, Y. Li, X. Xie, D. Katoshevski, Characterization of expiration air jets and droplet size distributions immediately at the mouth opening, J. Aerosol Sci. 40 (2009) 122–133, https://doi.org/10.1016/j.jaerosci.2008.10.003.

[44] A. Bouhuys, D.F. Proctor, J. Mead, Kinetic aspects of singing, J. Appl. Physiol. 21 (1966) 483–496, https://doi.org/10.1152/jappl.1966.21.2.483.

[45] G. Buonanno, L. Stabile, L. Morawska, Estimation of airborne viral emission: quanta emission rate of SARS-CoV-2 for infection risk assessment, Environ. Int. 141 (2020), 105794, https://doi.org/10.1016/j.envint.2020.105794.

[46] Fundamental factors affecting upper-room ultraviolet germicidal irradiation - part I. experimental - PubMed (n.d.), https://pubmed.ncbi.nlm.nih.gov/17365506/. (Accessed 6 January 2022).

[47] E.C. Riley, G. Murphy, R.L. Riley, Airborne spread of measles in a suburban elementary school, Am. J. Epidemiol. 107 (1978) 421–432, https://doi.org/10.1093/oxfordjournals.aje.a112560.

[48] C.B. Beggs, E.J. Avital, Upper-room ultraviolet air disinfection might help to reduce COVID-19 transmission in buildings: a feasibility study, PeerJ 8 (2020), e10196, https://doi.org/10.7717/peerj.10196.

[49] M. Raeiszadeh, B. Adeli, A critical review on ultraviolet disinfection systems against COVID-19 Outbreak: applicability, validation, and safety considerations, ACS Photonics 7 (2020) 2941–2951, https://doi.org/10.1021/acsphotonics.0c01245.

[50] G. Berry, A. Parsons, M. Morgan, J. Rickert, H. Cho, A review of methods to reduce the probability of the airborne spread of COVID-19 in ventilation systems and enclosed spaces, Environ. Res. 203 (2022), 111765, https://doi.org/10.1016/j.envres.2021.111765.

[51] M. First, S.N. Rudnick, K.F. Banahan, R.L. Vincent, P.W. Brickner, Fundamental factors affecting upper-room ultraviolet germicidal irradiation - part I. Experimental, J. Occup. Environ. Hyg. 4 (2007) 321–331, https://doi.org/10.1080/15459620701271693.

[52] Y. Yang, W.Y. Chan, C.L. Wu, R.Y.C. Kong, A.C.K. Lai, Minimizing the exposure of airborne pathogens by upper-room ultraviolet germicidal irradiation: an experimental and numerical study, J. R. Soc. Interface 9 (2012) 3184–3195, https://doi.org/10.1098/rsif.2012.0439.

[53] P. Xu, N. Fisher, S.L. Miller, Using computational Fluid Dynamics modeling to evaluate the design of hospital ultraviolet germicidal irradiation systems for inactivating airborne mycobacteria, Photochem. Photobiol. 89 (2013) 792–798, https://doi.org/10.1111/php.12062.

[54] S. Srivastava, X. Zhao, A. Manay, Q. Chen, Effective ventilation and air disinfection system for reducing coronavirus disease 2019 (COVID-19) infection risk in office buildings, Sustain. Cities Soc. 75 (2021), 103408, https://doi.org/10.1016/j.scs.2021.103408.

[55] R. Li, S. Pei, B. Chen, Y. Song, T. Zhang, W. Yang, J. Shaman, Substantial undocumented infection facilitates the rapid dissemination of novel coronavirus (SARS-CoV-2), Science 368 (2020) 489–493, https://doi.org/10.1126/science.abb3221.

[56] M. Abboah-Offei, Y. Salifu, B. Adewale, J. Bayuo, R. Ofosu-Poku, E.B.A. Opare-Lokko, A rapid review of the use of face mask in preventing the spread of COVID-19, Int. J. Nurs. Stud. Adv. 3 (2021), 100013, https://doi.org/10.1016/j.ijnsa.2020.100013.

[57] Y. Li, M. Liang, L. Gao, M. Ayaz Ahmed, J.P. Uy, C. Cheng, Q. Zhou, C. Sun, Face masks to prevent transmission of COVID-19: a systematic review and meta-analysis, Am. J. Infect. Control 49 (2021) 900–906, https://doi.org/10.1016/j.ajic.2020.12.007.

[58] M. Buonanno, D. Welch, I. Shuryak, D.J. Brenner, Far-UVC light (222 nm) efficiently and safely inactivates airborne human coronaviruses, Sci. Rep. 10 (2020), 10285, https://doi.org/10.1038/s41598-020-67211-2.

[59] D.H. Sliney, B.E. Stuck, A need to revise human exposure limits for ultraviolet UV-C radiation †, Photochem. Photobiol. 97 (2021) 485–492, https://doi.org/10.1111/php.13402.

[60] A Novel Coronavirus from Patients with Pneumonia in China, NEJM, 2019 (n.d.), https://www.nejm.org/doi/10.1056/NEJMoa2001017. (Accessed 13 January 2022).

[61] K.P. Fennelly, Particle sizes of infectious aerosols: implications for infection control, Lancet Respir. Med. 8 (2020) 914–924, https://doi.org/10.1016/S2213-2600(20)30323-4.